Acta Crystallographica Section F
Structural Biology and Crystallization Communications
ISSN 1744-3091

Crystallization and preliminary X-ray characterization of a catalytic and ATP-binding domain of a putative PhoR histidine kinase from the γ-radioresistant bacterium *Deinococcus radiodurans*

S. Caria,[a,b] D. de Sanctis,[a] F. J. Enguita[c]* and S. McSweeney[a]*

[a]Structural Biology Group, European Synchrotron Radiation Facility, France, [b]Faculty of Pharmacy, University of Lisbon, Portugal, and [c]Cell Biology Unit, Institute of Molecular Medicine, Faculty of Medicine, University of Lisbon, Portugal

Correspondence e-mail: fenguita@fm.ul.pt, mcsweeney@esrf.fr

Received 16 September 2009
Accepted 16 December 2009

The gene product of histidine kinase DR2244 (putative *pho*R) encoded by *Deinococcus radiodurans* has been suggested to be involved in the PhoR–PhoB two-component regulatory system. This two-component signalling system is activated upon phosphate starvation in several bacteria, including *D. radiodurans*. Single crystals were obtained from a recombinant preparation of the catalytic/ATP-binding (CA) domain of *D. radiodurans* PhoR (79–224) overexpressed in *Escherichia coli*. The crystals belonged to space group $P2_12_12_1$, with unit-cell parameters a = 46.9, b = 81.8, c = 204.6 Å. The crystals contained six molecules in the asymmetric unit. Diffraction data were collected to 2.4 Å resolution on beamline ID23-2 of the European Synchrotron Radiation Facility.

1. Introduction

Deinococcus radiodurans is a bacterium that is resistant to extreme conditions, including exposure to desiccation, UV light, high doses of ionizing radiation and numerous DNA-damaging chemical agents (Wang & Schellhorn, 1995; Minton, 1994). This microorganism is a nonpathogenic, Gram-positive, nonsporulating, nonmotile, spherical and obligate aerobe. Its genome is composed of a 2.64 Mbp chromosome, a 412 kbp chromosome, a 177 kbp megaplasmid and a 45 kbp plasmid and its genes have been annotated by analysis in *PSI-BLAST* (White *et al.*, 1999).

Two-component regulatory systems are widespread in nature as signal transduction systems that transport information on extracellular events (Stock *et al.*, 2000). The PhoR–PhoB system has been related to the cellular response to stress and to nutrient starvation. In *D. radiodurans*, several two-component systems have been characterized on the basis of sequence homology to systems that are present in other bacterial and eukaryotic cells. The response regulator PhoB was annotated as the gene DR2245 (*pho*B; White *et al.*, 1999). In the same operon, an adjacent gene (DR2244) encodes a putative PhoR histidine kinase.

The PhoR–PhoB system from *D. radiodurans* is thought to be involved in the signalling of extracellular phosphate concentration, being activated upon phosphate starvation. Models of this system have been proposed for *Escherichia coli* and *Bacillus subtilis*, but the mechanism of signal activation is not yet fully understood (Wanner, 1996; Van Dien & Keasling, 1998; Lamarche *et al.*, 2008). Upon phosphate starvation, the histidine kinase PhoR is activated *via* autophosphorylation on a histidine residue (His23 in *D. radiodurans* by homology). The phosphoryl group is then transferred to the aspartate (Asp52 in *D. radiodurans* by homology) of the response regulator PhoB. Upon phosphorylation, PhoB dimerizes, increasing its binding affinity for a conserved DNA sequence (*pho* box) and leading to the transcription of several genes. In *E. coli*, two-dimensional

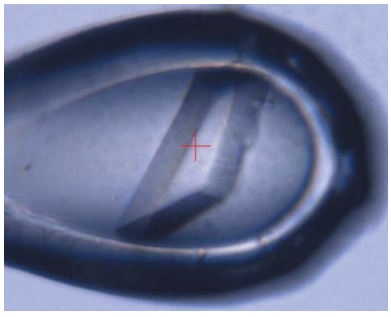

electrophoresis showed that the PhoB protein regulates 137 genes (VanBogelen *et al.*, 1996; Vershinina & Znamenskaia, 2002). This characterizes the Pho regulon, which leads to the expression of products that act in phosphorus metabolism or transport, namely PhoB, PstS, PhoA, PhnC and UgpB (Kimura *et al.*, 1989; Kasahara *et al.*, 1991; Makino *et al.*, 1991).

Several studies have been carried out to determine the mechanism by which PhoR receives the environmental stimulus. One of the first proposals was that it could interact with the PhoU protein from the phosphate-transport (Pst) system; however, the experimental data are not sufficient to support this hypothesis. It has been observed that the Pst system plays a role in this regulation, with PhoU being a negative regulator of the Pho system (Rice *et al.*, 2009).

The majority of histidine kinases (HKs) are multifunctional enzymes with autokinase, phosphotransfer and phosphatase activities and most of them are transmembrane sensor proteins (Grebe & Stock, 1999). Sensor HKs contain two domains: an N-terminal dimerization and histidine-phosphotransfer (DHp) domain and a C-terminal catalytic and ATP-binding (CA) domain (Grebe & Stock, 1999). The DHp domain, which contains the autophosphorylation site (a histidine residue), forms a stable dimer and can be phosphorylated by the CA domain in the presence of ATP (Grebe & Stock, 1999; Stock *et al.*, 2000; Khorchid & Ikura, 2006). Three-dimensional structures of histidine kinase DHp and CA domains have been reported and generally have a conserved secondary structure. The DHp domain consists of two α-helices that dimerize forming a four-helical bundle, while the CA domain presents a fold known as an α/β sandwich, which is composed of one layer consisting of a five-stranded β-sheet and another layer consisting of three α-helices (Song *et al.*, 2004; Marina *et al.*, 2005; Nowak *et al.*, 2006).

The PhoR CA domain is a polypeptide of 146 amino acids with a theoretical isoelectric point of 8.4 and a calculated molecular weight of 15 907 Da. The structures of related proteins from the Protein Data Bank, based on sequence similarity (Altschul *et al.*, 1997), are the histidine kinases from *Thermotoga maritima* (31% sequence identity; PDB code 2c2a; Marina *et al.*, 2005), *E. coli* (33% sequence identity; PDB code 1r62; Song *et al.*, 2004), *Mycobacterium tuberculosis* (33% sequence identity; PDB code 1ysr; E. Nowak, S. Panjikar & P. Tucker, unpublished work) and *Salmonella typhimurium* (27% sequence identity; PDB code 3cgy; Guarnieri *et al.*, 2008).

In this study, we describe the purification, overexpression, crystallization and preliminary X-ray analysis of the CA domain (79–224) of the putative PhoR (DR2244) from *D. radiodurans*, a member of the histidine-kinase family.

2. Experimental

2.1. Protein expression and purification

The DNA fragment containing amino acids 79–224 encoded by the DR2244 (putative *pho*R) gene was amplified from *D. radiodurans* genomic DNA by polymerase chain reaction (PCR) using complementary gene-specific primers (forward primer, CACCCGCACGCTGCCGCTGGCC; reverse primer, TCAGCCCAGCCCGCCCAC) and a high-fidelity PCR enzyme mix (Fermentas). An initial DNA-denaturation step was performed at 371 K for 5 min, followed by 30 cycles of 1 min at 368 K, 1 min at 328 K and 1 min at 345 K and a final 10 min extension cycle at 345 K. The blunt-end amplicons generated were then purified from the 1% agarose gel using a QIAquick gel-extraction kit (Qiagen). The fragment obtained was cloned into the pET151/D-TOPO vector using the TOPO cloning method (Invitrogen). The TOPO cloning vector added an N-terminal His_6 tag, a V5 epitope and a tobacco etch virus (TEV) protease cleavage site to the expressed recombinant protein. Recombinant clones were selected by ampicillin resistance and colony PCR analysis using the T7 promoter and double digestion with *Sac*I and *Nco*I (Fermentas) restriction enzymes to confirm the presence of a correctly sized insert. The integrity of the cloned CA domain of the *pho*R gene was confirmed by DNA sequencing.

The expression construct was transformed into chemically competent *E. coli* BL21 (DE3) cells (Invitrogen) using a heat-shock technique. A small overnight culture grown at 310 K in Luria–Bertani broth containing 100 µg ml^{-1} ampicillin was used to inoculate a 1 l culture. Cells were grown to an OD_{600} of 0.6. Expression of the recombinant protein was then induced by addition of isopropyl β-D-1-thiogalactopyranoside (IPTG) to a final concentration of 0.3 m*M*. After 3 h induction at 298 K, the cells were harvested by centrifugation at 5000*g* for 30 min at 277 K. Subsequently, they were frozen at 193 K, thawed and then resuspended in 50 m*M* Tris–HCl buffer pH 7 containing 0.5 *M* NaCl (buffer *A*). Lysis was performed by three cycles of freezing (liquid nitrogen) and thawing (293 K water bath).

A 1 ml HisTrap FF Column (GE Healthcare) equilibrated with buffer *A* containing 20 m*M* imidazole was attached to an ÄKTA Prime system (GE Healthcare). The soluble fraction was applied onto the column and washed with 30 ml of the same buffer followed by a 25 ml wash with buffer *A* containing 50 m*M* imidazole. The target protein was eluted with a linear gradient of imidazole (from 50 to

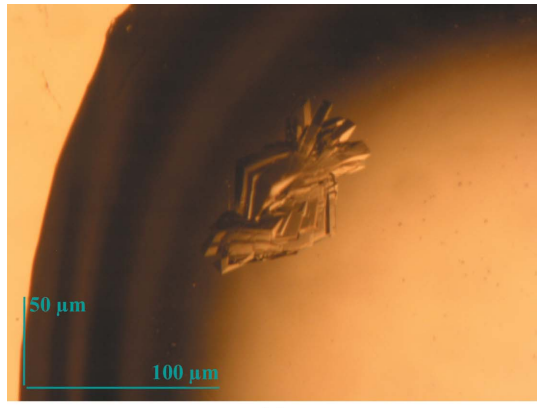

(*a*)

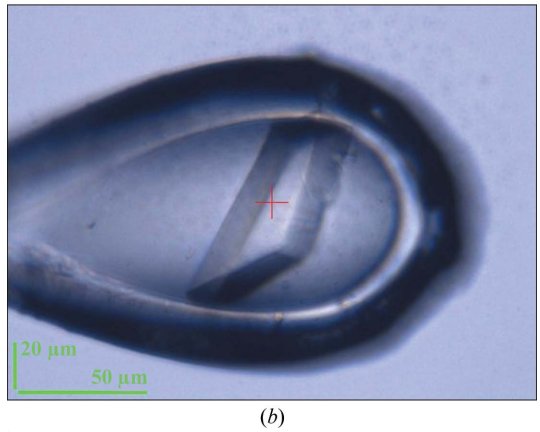

(*b*)

Figure 1
PhoR histidine kinase CA domain (PhoR-CA) crystals grown at 287 K in 0.1 *M* Tris–HCl pH 8.8 with 14%(*w*/*v*) PEG 4000 and 0.2 *M* $MgCl_2$. (*a*) PhoR-CA crystals obtained in 3 d in a drop set up manually in a 24-well plate using the hanging-drop vapour-diffusion method. (*b*) PhoR-CA crystal obtained after 2 d in a drop set up manually in a 24-well plate using the hanging-drop vapour-diffusion method with streak-seeding from the crystals in (*a*). The crystal is mounted in a 100 µm loop on ID23-2.

Table 1
Diffraction data-processing statistics.

Values in parentheses are for the highest resolution shell.

Source	ESRF ID23-2
Detector	MAR Mosaic 225 CCD
Space group	$P2_12_12_1$
Unit-cell parameters (Å)	a = 46.9, b = 81.8, c = 204.6
Wavelength (Å)	0.8726
No. of unique intensities	31476 (4495)
Redundancy	4.4 (4.5)
Resolution (Å)	43.27–2.4 (2.53–2.4)
Completeness (%)	99.7 (99.4)
$R_{\rm merge}$† (%)	11 (35.4)
$R_{\rm p.i.m.}$‡ (%)	6 (19.3)
$I/\sigma(I)$	5.7 (2.0)
Mean $I/\sigma(I)$	11.6 (5.2)

† $R_{\rm merge} = \sum_{hkl}\sum_i |I_i(hkl) - \langle I(hkl)\rangle| / \sum_{hkl}\sum_i I_i(hkl)$. ‡ $R_{\rm p.i.m.} = \sum_{hkl}[1/(N-1)]^{1/2} \times \sum_i |I_i(hkl) - \langle I(hkl)\rangle| / \sum_{hkl}\sum_i I_i(hkl)$.

500 m*M* in six column volumes) in buffer *A*. Fractions containing the PhoR CA domain (PhoR-CA) were identified by SDS–PAGE analysis and dialysed overnight at 277 K in the presence of TEV protease in a 1:6 ratio into 20 m*M* Tris–HCl buffer pH 7 containing 150 m*M* NaCl, 1 m*M* DTT and 0.5 m*M* EDTA. The amino-acid sequence that remained in the protein sequence after TEV cleavage was GIDPFT. The protein mixture was reloaded onto a 1 ml HisTrap FF Column (GE Healthcare) and the flowthrough was collected. Fractions containing untagged PhoR-CA were identified by SDS–PAGE, pooled and dialysed with 20 m*M* Tris–HCl buffer pH 7 containing 150 m*M* NaCl.

The protein was concentrated to 6 mg ml^{-1} using a 3 kDa molecular-weight cutoff Amicon concentrator (Millipore). The protein concentration was estimated from the absorption at 280 nm using a calculated extinction coefficient of 19 480 M^{-1} cm^{-1}. The sample purity was estimated to be about 95% by SDS–PAGE.

2.2. Crystallization

Initial crystallization screening was carried out manually at 295 K using the hanging-drop vapour-diffusion method in 24-well plates with PhoR-CA at 6 mg ml^{-1} in 20 m*M* Tris–HCl buffer pH 7 containing 150 m*M* NaCl. Crystallization screens from Hampton Research (Sodium Malonate Grid Screen and Crystal Screens I and II) were used. The 3 µl drop (containing a 1:1 ratio of protein and reservoir solution) was equilibrated against 500 µl reservoir solution.

Crystals of PhoR-CA were obtained within 1–2 d in two conditions from Crystal Screens I and II. These were reproduced using stock solutions, keeping the same drop size, in 24-well sitting-drop plates at 293 K. The crystallization condition that yielded the crystals that diffracted X-rays to the highest resolution was 0.1 *M* Tris–HCl pH 8.5, 30%(*w*/*v*) PEG 4000 and 0.2 *M* $MgCl_2$; unfortunately, these crystals exhibited multiple diffraction patterns to a resolution of 3.5 Å. Further optimization yielded single crystals. The best diffraction-quality crystals were grown from a solution consisting of 0.1 *M* Tris–HCl pH 8.8, 14%(*w*/*v*) PEG 4000 and 0.2 *M* $MgCl_2$. Streak-seeding and incubation at 287 K were essential factors for obtaining single well shaped crystals. Using this process, the clusters of very thin plate-shaped crystals obtained directly from Crystal Screen I at 293 K were replaced by larger multiple crystals (Fig. 1*a*) grown at 287 K, which were optimized to produce single crystals (Fig. 1*b*).

2.3. Cryoprotection of the crystals

Single crystals were transferred to stabilization solution [0.1 *M* Tris–HCl pH 8.8, 17%(*w*/*v*) PEG 4000 and 0.2 *M* $MgCl_2$] previously incubated at 287 K. Crystals were cryoprotected by adding 20% glycerol to this solution and incubating the solution at 287 K. The crystals proved to be very sensitive to temperature variation and their diffraction quality was affected. For this reason, all crystal manipulation was performed at 287 K.

2.4. Data collection

Several data sets were collected using synchrotron radiation on the Macromolecular Crystallography beamlines at the ESRF, Grenoble (Table 1). The highest resolution diffraction data were obtained from a crystal with dimensions 100 × 50 × 5 µm that was flash-cooled in liquid nitrogen and were measured on the ID23-2 beamline of the ESRF. Diffraction data were collected at 100 K using an Oxford Cryostream. Diffraction images were integrated with *iMOSFLM* (Leslie, 2006) and were scaled using *SCALA* (Evans, 2006) from the *CCP*4 suite (Collaborative Computational Project, Number 4, 1994). Examination of diffraction data and systematic absences indicated that the space group was $P2_12_12_1$.

3. Results and discussion

The DNA fragment encoding the catalytic domain of the PhoR histidine-kinase gene from *D. radiodurans* (PhoR-CA) was successfully cloned in *E. coli* and the encoded hexahistidine-tagged PhoR-CA was purified to homogeneity by metal-chelating affinity chromatography. Diffraction-quality crystals typically appeared in 2–5 d. The crystals suffered greatly upon freezing and a number of cryoprotection strategies were attempted. The most successful cryoprotection was obtained by using a stabilization solution with a higher PEG concentration and then adding 20% glycerol to the previous solution. The most important step in the cryocooling procedure was to incubate all solutions used during the process at 287 K for 2 h before freezing the crystals. Data collection was optimized taking radiation damage into account by using *EDNA* to determine the best strategy (http://www.edna-project.org). Structure solution by molecular replacement (MR) is currently under way using homologous structures present in the PDB.

We thank Joanna Timmins, Laurent Terradot and the ESRF MX group for suggestions during the project and for access to ESRF beamlines. This work is part of an ongoing in-house research project in the ESRF Macromolecular Crystallography Group and was funded by an ESRF PhD stipend to SC.

References

Altschul, S. F., Madden, T. L., Schäffer, A. A., Zhang, J., Zhang, Z., Miller, W. & Lipman, D. J. (1997). *Nucleic Acids Res.* **25**, 3389–3402.
Collaborative Computational Project, Number 4 (1994). *Acta Cryst.* D**50**, 760–763.
Evans, P. (2006). *Acta Cryst.* D**62**, 72–82.
Grebe, T. W. & Stock, J. B. (1999). *Adv. Microb. Physiol.* **41**, 139–227.
Guarnieri, M. T., Zhang, L., Shen, J. & Zhao, R. (2008). *J. Mol. Biol.* **379**, 82–93.
Kasahara, M., Makino, K., Amemura, M., Nakata, A. & Shinagawa, H. (1991). *J. Bacteriol.* **173**, 549–558.
Khorchid, A. & Ikura, M. (2006). *Int. J. Biochem. Cell Biol.* **38**, 307–312.
Kimura, S., Makino, K., Shinagawa, H., Amemura, M. & Nakata, A. (1989). *Mol. Gen. Genet.* **215**, 374–380.
Lamarche, M. G., Wanner, B. L., Crepin, S. & Harel, J. (2008). *FEMS Microbiol. Rev.* **32**, 461–473.
Leslie, A. G. W. (2006). *Acta Cryst.* D**62**, 48–57.
Makino, K., Kim, S.-K., Shinagawa, H., Amemura, M. & Nakata, A. (1991). *J. Bacteriol.* **173**, 2665–2672.

Marina, A., Waldburger, C. D. & Hendrickson, W. A. (2005). *EMBO J.* **24**, 4247–4259.
Minton, K. W. (1994). *Mol. Microbiol.* **13**, 9–15.
Nowak, E., Panjikar, S., Morth, J. P., Jordanova, R., Svergun, D. I. & Tucker, P. A. (2006). *Structure*, **14**, 275–285.
Rice, C. D., Pollard, J. E., Lewis, Z. T. & McCleary, W. R. (2009). *Appl. Environ. Microbiol.* **75**, 573–582.
Song, Y., Peisach, D., Pioszak, A. A., Xu, Z. & Ninfa, A. J. (2004). *Biochemistry*, **43**, 6670–6678.
Stock, A. M., Robinson, V. L. & Goudreau, P. N. (2000). *Annu. Rev. Biochem.* **69**, 183–215.
VanBogelen, R. A., Olson, E. R., Wanner, B. L. & Neidhardt, F. C. (1996). *J. Bacteriol.* **178**, 4344–4366.
Van Dien, S. J. & Keasling, J. D. (1998). *J. Theor. Biol.* **190**, 37–49.
Vershinina, O. A. & Znamenskaia, L. V. (2002). *Mikrobiologiia*, **71**, 581–595.
Wang, P. & Schellhorn, H. E. (1995). *Can. J. Microbiol.* **41**, 170–176.
Wanner, B. L. (1996). *Kidney Int.* **49**, 964–967.
White, O. *et al.* (1999). *Science*, **286**, 1571–1577.